

## Effect of $\text{La}_2\text{O}_3/\text{CeO}_2$ particle size on high-temperature oxidation resistance of electrodeposited $\text{Ni-La}_2\text{O}_3/\text{CeO}_2$ composites

Jun-sheng MENG<sup>1,2</sup>, Ze-sheng JI<sup>2</sup>

1. College of Materials Science and Engineering, Heilongjiang University of Science and Technology, Harbin 150022, China;
2. College of Materials Science and Engineering, Harbin University of Science and Technology, Harbin 150040, China

Received 13 November 2013; accepted 10 April 2014

**Abstract:**  $\text{Ni-La}_2\text{O}_3/\text{CeO}_2$  composite films were prepared by electrodeposition from a nickel sulfate bath containing certain content of micrometer and nanometer  $\text{La}_2\text{O}_3/\text{CeO}_2$  particles. The effect of  $\text{La}_2\text{O}_3$  or  $\text{CeO}_2$  particle size on the oxidation resistance of the electrodeposited  $\text{Ni-La}_2\text{O}_3/\text{CeO}_2$  composites in air at 1000 °C was studied. The results indicate that, compared with the electrodeposited Ni-film,  $\text{Ni-La}_2\text{O}_3/\text{CeO}_2$  composites exhibit a superior oxidation resistance due to the codeposited  $\text{La}_2\text{O}_3$  or  $\text{CeO}_2$  particles blocking the outward diffusion of nickel. Moreover, compared with nanoparticles,  $\text{La}_2\text{O}_3$  or  $\text{CeO}_2$  microparticles have stronger effect because  $\text{La}_2\text{O}_3$  or  $\text{CeO}_2$  microparticles also act as a diffusion barrier layer at the onset of oxidation.

**Key words:** Ni-based composite; electrodeposition; high-temperature oxidation;  $\text{La}_2\text{O}_3$ ;  $\text{CeO}_2$ ; reactive element effect; oxidation mechanism

### 1 Introduction

Electrodeposition is a low-cost and low-temperature method suitable for producing metal matrix composite materials [1–3], which have potential applications in the aerospace industry due to their high temperature oxidation resistance [4,5]. In this process, fine particles or whiskers are suspended in the electrolyte and embedded in the growing metal layer. Recently, a considerable amount of research effort has been put into electrodeposition of Ni-based composite. With the codeposition of small amount of reactive elements oxides, such as  $\text{Y}_2\text{O}_3$ ,  $\text{CeO}_2$  and  $\text{La}_2\text{O}_3$ , the oxidation resistance of Ni film can be further improved [4–9] because the rapid outward diffusion of Ni along the grain boundary was inhibited mainly by segregated RE ions. The phenomenon was first reported in 1937 [10] and was referred to as “reactive element effect (REE)”. Various theories to elucidate the REE have been put forward but still are in dispute because the mechanism may differ for different oxide/RE systems [11,12]. PENG et al [4,5] further confirmed that only when  $\text{La}_2\text{O}_3$  particles are

small enough, they may act as a source of La ions by solution at high temperature to block the outward diffusion of Ni. The results were supported by works of CZERWINSKI et al [13,14], who proved that the addition of a sol-gel coating of ceria particles below 10 nm onto a nickel surface retarded the oxidation; however, when the size of  $\text{CeO}_2$  particles increased over some size limit by sintering and coarsening, the oxidation of nickel actually increased. Recently, ZHOU et al [9] have found that the codeposited  $\text{Y}_2\text{O}_3$  microparticles could significantly improve the oxidation resistance of Ni film because the re-precipitation of some  $\text{Y}_2\text{O}_3$  nanoparticles along the grain boundaries blocked the outward diffusion of Ni and changed its oxidation mechanism. It seems that the codeposited RE oxide microparticles should have the same effect as the nanoparticles counterpart. In view of current production cost and commercial availability of RE oxide nanoparticles, the application of microparticles rather than nanoparticles to electroplate oxidation-resistant Ni-film is of great interest from the point of engineering view. Therefore, it is useful to know the effect of RE oxide particle size on the oxidation of Ni films.

**Foundation item:** Project (GC13A113) supported by the Technology Research and Development Program of Heilongjiang Provincial Science and Technology Department; Project (12511469) supported by Heilongjiang Provincial Science and Technology Department

**Corresponding author:** Jun-sheng MENG; Tel: +86-451-88036695; E-mail: [mengjs2008@live.cn](mailto:mengjs2008@live.cn)

DOI: 10.1016/S1003-6326(14)63503-2

However, there has been no report about these yet. Previous works [4–7] also indicated that, in order to improve the oxidation resistance, the addition of a certain content of RE oxide nanoparticles is necessary. Lower content can not supply enough RE ions in short time to block the outward diffusion of Ni, while higher content even accelerates the oxidation of Ni film. XU et al [7] found 2.7% CeO<sub>2</sub> (mass fraction) nanoparticles could improve the oxidation of Ni-film. PENG et al [4,5] reported that 8.2% La<sub>2</sub>O<sub>3</sub> (mass fraction) particles could also improve the oxidation of Ni-film. In this work, nickel composites with (6.5±0.5)% La<sub>2</sub>O<sub>3</sub> or (4.5±0.4)% CeO<sub>2</sub> were chosen for the oxidation experiment to investigate the effect of RE oxide (La<sub>2</sub>O<sub>3</sub> or CeO<sub>2</sub>) particle size on the oxidation resistance of electrodeposited Ni–La<sub>2</sub>O<sub>3</sub>/CeO<sub>2</sub> composites.

## 2 Experimental

Pure nickel specimens with dimensions of 15 mm×10 mm×2mm were cut from a pure electrolytic nickel plate and then were abraded with 800# grit SiC waterproof paper. After being ultrasonically cleaned in acetone, the specimens were electrodeposited with (on all sides) a 20–55 μm-thick film of Ni–La<sub>2</sub>O<sub>3</sub> or Ni–CeO<sub>2</sub> composite from a nickel sulfate bath containing 150 g/L NiSO<sub>4</sub>·7 H<sub>2</sub>O, 15 g/L NH<sub>4</sub>Cl, 15 g/L H<sub>3</sub>BO<sub>3</sub>, 0.1 g/L C<sub>12</sub>H<sub>25</sub>NaSO<sub>4</sub>, and 25 g/L pure La<sub>2</sub>O<sub>3</sub> or CeO<sub>2</sub> particles, respectively. The mean diameters of micrometer La<sub>2</sub>O<sub>3</sub> and CeO<sub>2</sub> particles were 1.5 and 2.5 μm, respectively. The mean diameters of nanometer La<sub>2</sub>O<sub>3</sub> and CeO<sub>2</sub> particles are 80 and 10 nm, respectively. Electrodeposition was conducted in 1000 mL beaker at a current density of 3 A/dm<sup>2</sup>, temperature of 35 °C and pH value of 5.5–6.0. During the electrodeposition, magnetic stirring was employed to maintain the uniform particles concentration and prevent the sedimentation. The detailed coating process could be found elsewhere [4,5]. For comparison, a 55 μm-thick Ni film was also deposited under the same parameters in the same bath but without adding any La<sub>2</sub>O<sub>3</sub> or CeO<sub>2</sub> particles.

The isothermal oxidation experiments were carried out in air at 1000 °C for 20 h. The mass measurements were conducted after fixed time intervals using a balance with a sensitivity of 0.01 mg. The composition and phases of the as-deposited films before and after oxidation were investigated using a Camscan MX2600FE type scanning electron microscope (SEM) with energy dispersive X-ray spectroscopy (EDS) and D/Max–2500 pc type X-ray diffraction (XRD). The average nominal La<sub>2</sub>O<sub>3</sub> or CeO<sub>2</sub> concentrations were determined by using the La or Ce to oxygen ratio according to its chemical formula at 1000 magnification. Ten replicate tests at different locations were carried out

so as to minimize data scattering, and every value reported was an average of ten measurements. Electroless Ni-plating was plated on the surface of the oxidized specimens to prevent the spallation of the scales for observing cross-sections.

## 3 Results

A regular pyramidal structure as shown in Fig. 1(a) is observed on the surface of the Ni film due to a typical Ni growth texture [15]. However, with the addition of La<sub>2</sub>O<sub>3</sub> or CeO<sub>2</sub> particles, the grain size is significantly reduced and the morphology is changed to hemispherical grain structure except the one with CeO<sub>2</sub> microparticles, which have a nodular grain structure, as seen in Figs. 1(b) and (d). EDS results show that both the as-deposited Ni–La<sub>2</sub>O<sub>3</sub> composites contain (6.5±0.5)% La<sub>2</sub>O<sub>3</sub> (mass fraction) and the as-deposited Ni–CeO<sub>2</sub> composites contain (4.5±0.4)% CeO<sub>2</sub> (mass fraction). Although the distribution of bright La<sub>2</sub>O<sub>3</sub> or CeO<sub>2</sub> microparticles can be observed in some locations, the particles are not present in most areas, the same as the previous reports [4,5]. At the same time, lots of La<sub>2</sub>O<sub>3</sub> microparticles and CeO<sub>2</sub> nanoparticles form agglomerate clusters, as shown in Figs. 1(c) and (e). Figure 2 shows the cross sectional morphologies of the as-deposited Ni–La<sub>2</sub>O<sub>3</sub> and Ni–CeO<sub>2</sub> nanocomposites with a thickness of about 20 μm. The EDS results show that the white spots are enriched in La or Ce, implying that the deposited La<sub>2</sub>O<sub>3</sub> or CeO<sub>2</sub> nanoparticles are partially agglomerated.

The oxidation kinetics of various samples at 1000 °C for 20 h is illustrated in Fig. 3 as linear plots (Fig. 3(a)) and parabolic plots (Fig. 3(b)), respectively. At 1000 °C, all samples obey the parabolic rate law to a good approximation for the whole duration of the test. The calculated parabolic rate constants are listed in Table 1. It is obvious that the addition of La<sub>2</sub>O<sub>3</sub> or CeO<sub>2</sub> particles improves the oxidation resistance of Ni film. However, La<sub>2</sub>O<sub>3</sub> or CeO<sub>2</sub> microparticles have stronger effect to decrease the oxidation rate of Ni. From Table 1, it can be found that, compared with La<sub>2</sub>O<sub>3</sub> particles, CeO<sub>2</sub> particles have stronger effect.

XRD analysis shows that the scales formed on all samples are NiO. Figure 4 shows the surface morphologies of various samples after oxidation. Faceted NiO grains with the mean grain size of around 10 μm appear on the Ni film, as seen in Fig. 4(a). However, the NiO crystals formed on the Ni–La<sub>2</sub>O<sub>3</sub> or CeO<sub>2</sub> composites are fine grains, especially the composites with La<sub>2</sub>O<sub>3</sub> or CeO<sub>2</sub> microparticles, as seen in Figs. 4(c) and (d). From Fig. 4(b), it can be found that the scales are also somewhat convoluted. From the corresponding cross-section, the scales formed on Ni film exhibit a double-layer structure with a similar thickness: a

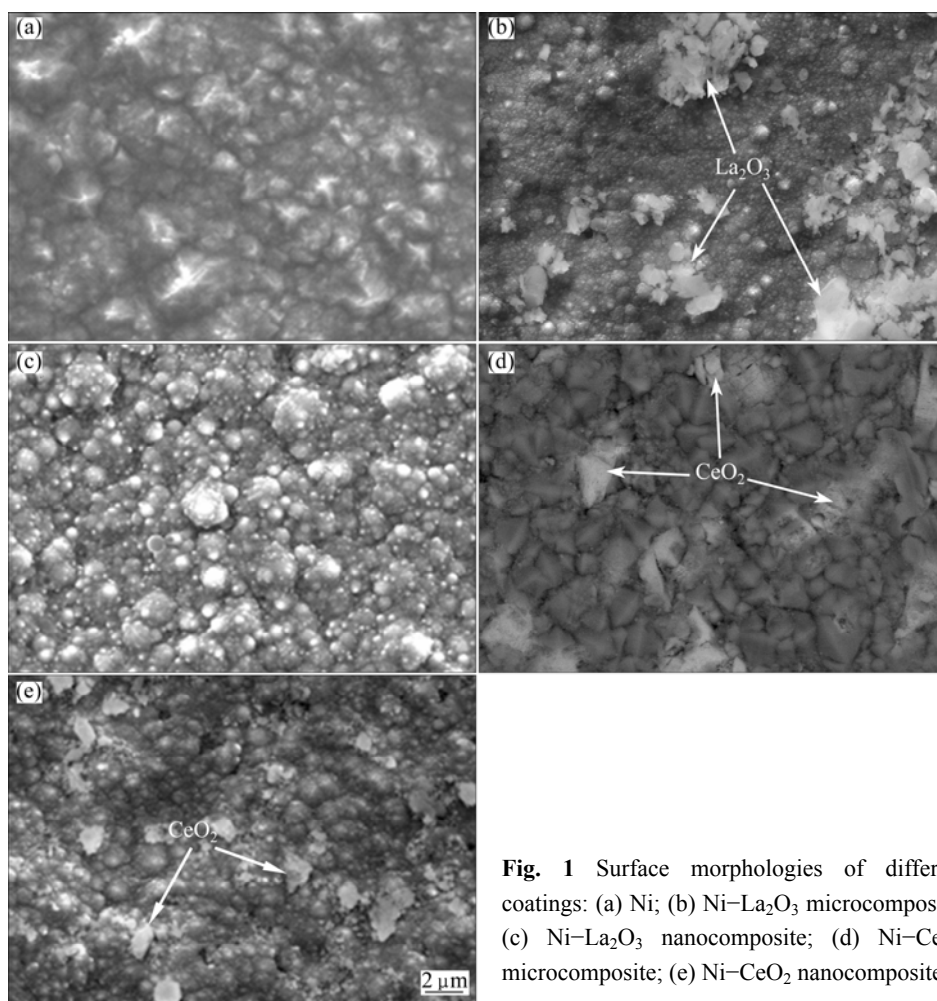


**Fig. 1** Surface morphologies of different coatings: (a) Ni; (b) Ni-La<sub>2</sub>O<sub>3</sub> microcomposite; (c) Ni-La<sub>2</sub>O<sub>3</sub> nanocomposite; (d) Ni-CeO<sub>2</sub> microcomposite; (e) Ni-CeO<sub>2</sub> nanocomposite

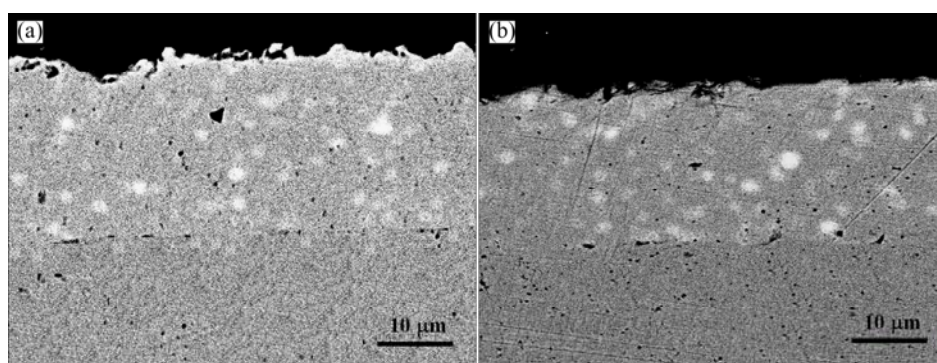


**Fig. 2** Cross-sectional morphologies of as-deposited Ni-La<sub>2</sub>O<sub>3</sub> (a) and Ni-CeO<sub>2</sub> (b) nanocomposites

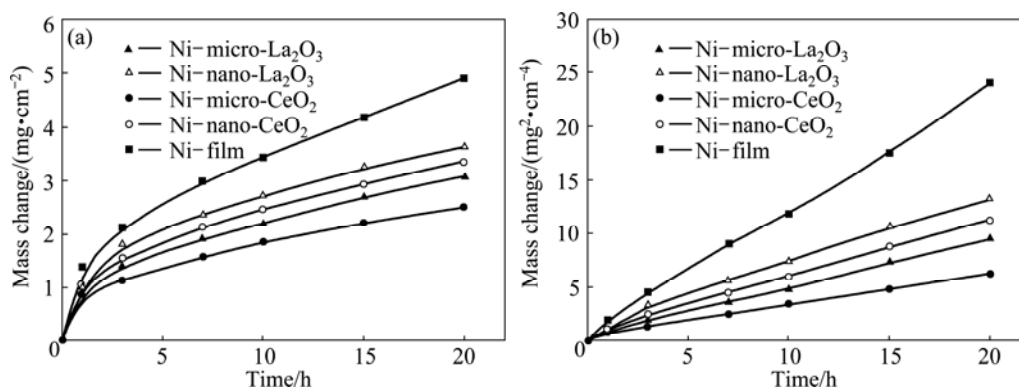


**Fig. 3** Dependence of mass change vs time for various samples oxidized at 1000 °C for 20 h: (a) Linear plot; (b) Parabolic plot

**Table 1** Calculated oxidation parabolic rate constants for samples oxidized at 1000 °C for 20 h

Sample	Parabolic rate constant/ ( $10^{-10} \text{g}^2 \cdot \text{cm}^{-4} \cdot \text{s}^{-1}$ )
Ni film	3.35
Ni-nano-CeO <sub>2</sub>	1.57
Ni-micro-CeO <sub>2</sub>	0.87
Ni-nano-La <sub>2</sub> O <sub>3</sub>	1.84
Ni-micro-La <sub>2</sub> O <sub>3</sub>	1.31

relatively coarse-grained, columnar outer layer and a more fine-grained inner layer, as seen in Fig. 5(a). However, the scale formed on Ni-La<sub>2</sub>O<sub>3</sub> or CeO<sub>2</sub> composites is thinner, in which bright oxide particles can be observed. EDS results show that the bright oxides are La- or Ce-enriched La<sub>2</sub>O<sub>3</sub> or CeO<sub>2</sub> phases. Due to its immovability compared with Ni, La<sub>2</sub>O<sub>3</sub> or CeO<sub>2</sub> particles can act as an inert marker. Thus, the scales without the dispersion of La<sub>2</sub>O<sub>3</sub> or CeO<sub>2</sub> particles below the oxide surface can be seen as the outer layer due to outward diffusion of Ni; the scales with dispersion of La<sub>2</sub>O<sub>3</sub> or

CeO<sub>2</sub> particles below outer layer can be seen as the inner layer due to inward diffusion of oxygen. From Fig. 5, it can be found that the oxidation of Ni-La<sub>2</sub>O<sub>3</sub>/CeO<sub>2</sub> composites is mainly controlled by the inward transport of oxygen, especially the composites with La<sub>2</sub>O<sub>3</sub> or CeO<sub>2</sub> microparticles, as seen in Figs. 5(b) and (d). The results suggest that La<sub>2</sub>O<sub>3</sub> or CeO<sub>2</sub> microparticles have stronger effect to block the outward diffusion of Ni.

## 4 Discussion

The oxidation behaviors of nickel have been studied in details and a relatively clear understanding of these processes has been attained [4–7]. At 1000 °C, the reported growth kinetics of NiO scales is parabolic and interpreted on the basis of Wagner's theory [16]. The scales grown at this temperature are characterized by a duplex scale formed on a porous and fine equiaxed grain inner layer due to the inward diffusion of oxygen to the scale/metal interface through discontinuous short-circuit paths, such as voids, microchannels, and fissures in the outer oxide scale, and a more compact and coarser

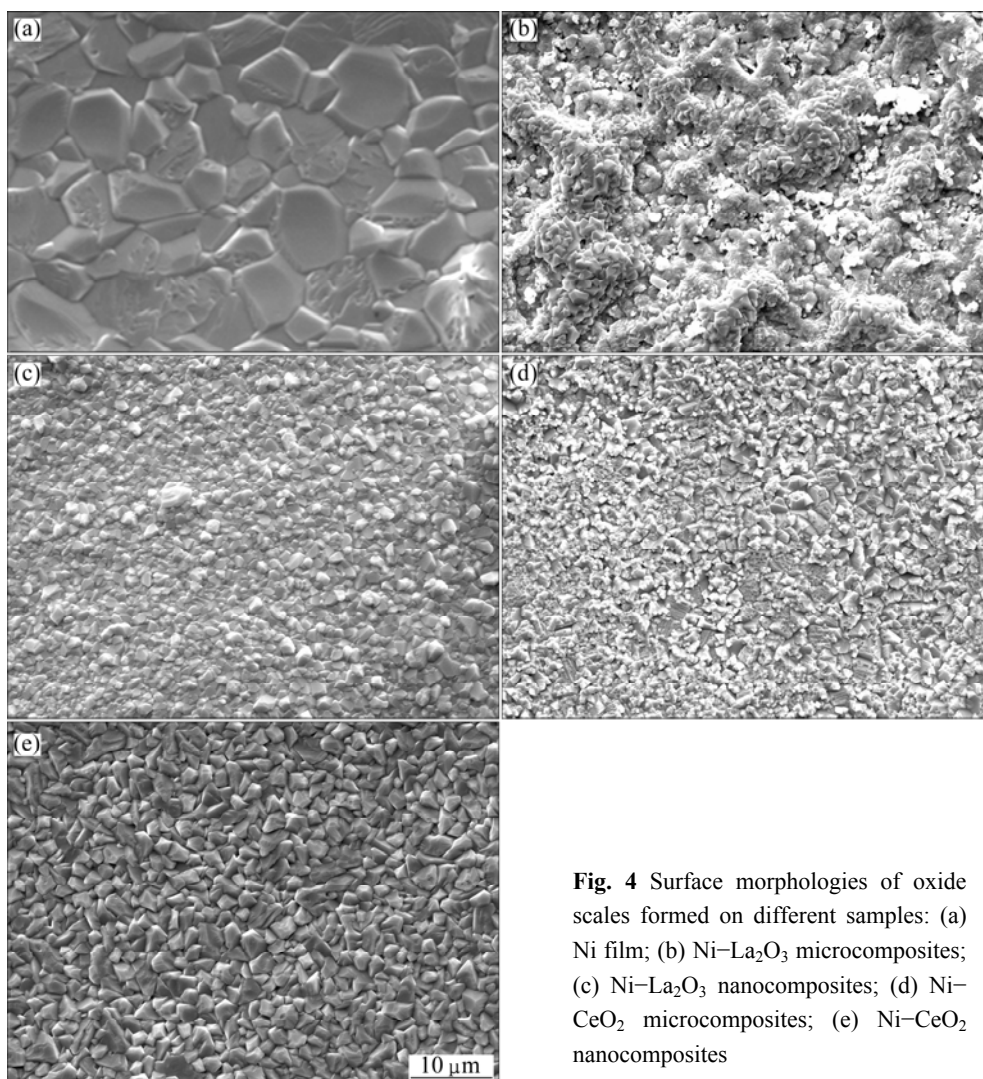


**Fig. 4** Surface morphologies of oxide scales formed on different samples: (a) Ni film; (b) Ni-La<sub>2</sub>O<sub>3</sub> microcomposites; (c) Ni-La<sub>2</sub>O<sub>3</sub> nanocomposites; (d) Ni-CeO<sub>2</sub> microcomposites; (e) Ni-CeO<sub>2</sub> nanocomposites

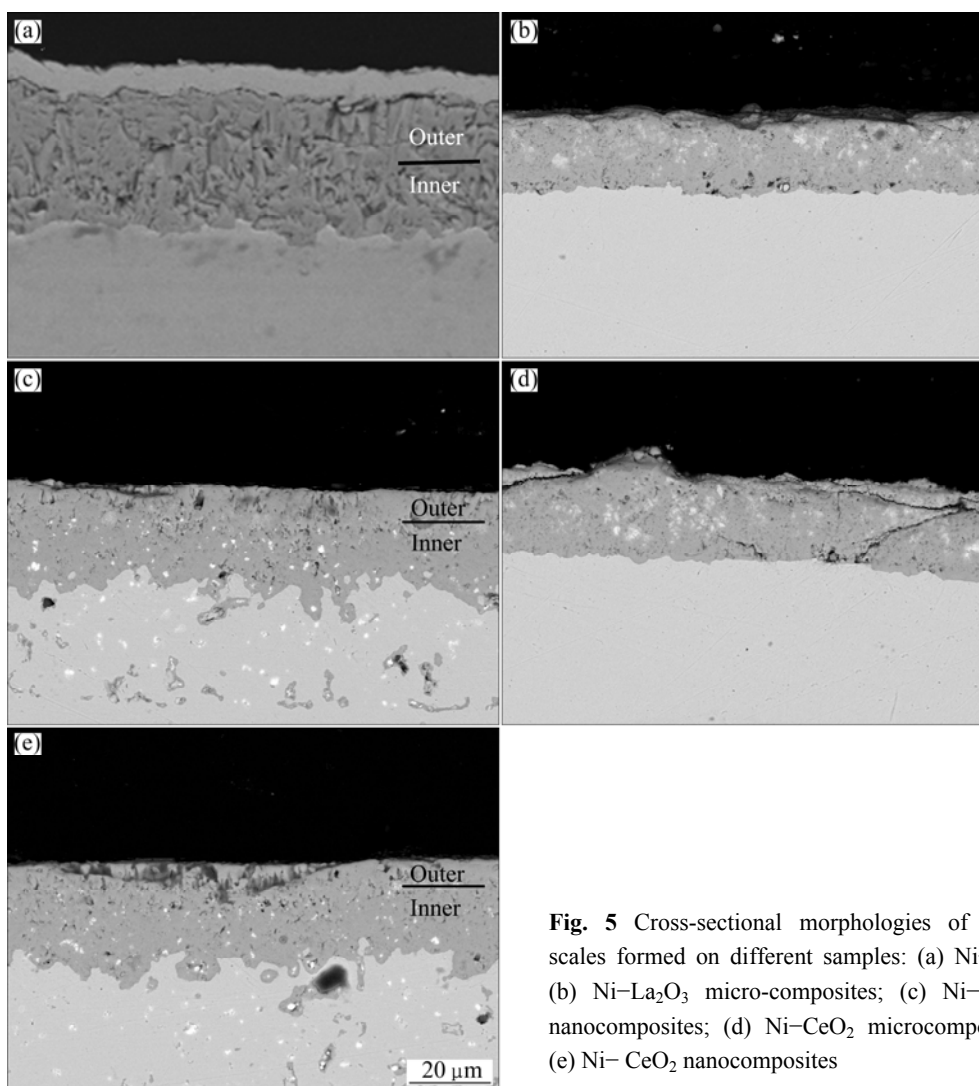


**Fig. 5** Cross-sectional morphologies of oxide scales formed on different samples: (a) Ni-film; (b) Ni-La<sub>2</sub>O<sub>3</sub> micro-composites; (c) Ni-La<sub>2</sub>O<sub>3</sub> nanocomposites; (d) Ni-CeO<sub>2</sub> microcomposites; (e) Ni-CeO<sub>2</sub> nanocomposites

columnar outer layer due to the outward diffusion of nickel along grain boundaries [17–20]. According to the experimental results, the formation of duplex scale with a similar thickness on Ni film suggests that both the inward diffusion of oxygen and outward diffusion of Ni have a similar effect for the oxidation of Ni film. With the addition of La<sub>2</sub>O<sub>3</sub> or CeO<sub>2</sub> nanoparticles, the oxidation resistance is further improved because the rapid outward diffusion of Ni along the grain boundary is inhibited to a great extent. The reasons are addressed below. As the oxidation starts, the formation of outer NiO will quickly sweep the La<sub>2</sub>O<sub>3</sub> or CeO<sub>2</sub> nanoparticles on/adjacent to the surface. After the transient stage of the oxidation, an oxygen potential gradient is established in the metal–scale–gas system and the RE addition begins to take effect on the scale according to “dynamic-segregation theory” [12]. RE ions from the added RE or its oxides by the dissolution first segregate to metal/scale interface and then to the gas/scale interface through the scale grain boundaries. When the concentration of RE ions at the scale grain boundaries reaches a critical value,

the segregation diffusion of RE ions blocks the outward diffusion of Ni and results in scale growth controlled primarily by the inward diffusion of oxygen. However, experimental evidence for the assumption has been still lacking. Since RE oxides are relatively immobile and can be regarded as inert remarks compared with Ni, the columnar outer layer/fine equiaxed inner layer interfaces correspond approximately to the original Ni-La<sub>2</sub>O<sub>3</sub>/CeO<sub>2</sub> composite coating surface. With the oxidation progress, more La<sub>2</sub>O<sub>3</sub> or CeO<sub>2</sub> particles incorporate into NiO because its inward growth may also dissolve, producing La/Ce ions segregated to the oxide grain boundaries, and thus preventing the reduction of La/Ce concentration at the grain boundaries during a long oxidation time. At the same time, pinning [21] and “solute-drag” effect [12] of the dispersion particles at oxide grain boundaries give rise to the formation of fine oxide grains. This may be the direct evidence that La/Ce segregates to the scale grain boundaries. However, for the oxidation of Ni-La<sub>2</sub>O<sub>3</sub>/CeO<sub>2</sub> composite with La<sub>2</sub>O<sub>3</sub>/CeO<sub>2</sub> microparticles, NiO scales should grow faster at the

onset of the oxidation because it needs more time to dissolve enough La or Ce ions to block the outward diffusion of Ni. The case, however, is not observed from the oxidation kinetics and scale structure. The fact is that the growth rate of NiO scale is noticeably retarded at the onset of the oxidation and a finer grain NiO scale with a thicker inner layer forms. The only reason lies that the outward growth of NiO is inhibited at the onset of the oxidation. Recent works [22–25] show that the CeO<sub>2</sub> or La<sub>2</sub>O<sub>3</sub> layers have a similar effect as the diffusion barrier layer to block the outward diffusion of Ni. In this experiment, La<sub>2</sub>O<sub>3</sub> or CeO<sub>2</sub> microparticles on the composite surface may also have a similar effect to block the outward diffusion of Ni. Due to its larger size and higher content on the surface, a lower scaling rate occurs. With the oxidation progress, La<sub>2</sub>O<sub>3</sub> or CeO<sub>2</sub> microparticles begin to incorporate into NiO. After they dissolve and segregate to the oxide grain boundaries, they begin to take REE as like nanoparticles counterpart.

## 5 Conclusions

1) The codeposition of La<sub>2</sub>O<sub>3</sub> or CeO<sub>2</sub> particles changes the direction of Ni growth and causes the formation of a finer grain structure.

2) The inward diffusion of oxygen controls the oxidation progress of Ni–La<sub>2</sub>O<sub>3</sub>/CeO<sub>2</sub> composite due to La<sub>2</sub>O<sub>3</sub> or CeO<sub>2</sub> particles blocking the outward diffusion of Ni.

3) Compared with La<sub>2</sub>O<sub>3</sub> or CeO<sub>2</sub> nanoparticles, La<sub>2</sub>O<sub>3</sub> or CeO<sub>2</sub> microparticles have stronger effect to decrease the oxidation rate of Ni because La<sub>2</sub>O<sub>3</sub> or CeO<sub>2</sub> microparticles also act as a diffusion barrier layer at the onset of the oxidation.

## References

- [1] TUSHAR B, SANDIP P H. Effect of electrodeposition conditions and reinforcement content on microstructure and tribological properties of nickel composite coatings [J]. *Surface and Coatings Technology*, 2011, 205: 4124–4134.
- [2] ARUNA S T, WILLIAN GRIPS V K, RAJAM K S. Ni-based electrodeposited composite coating exhibiting improved microhardness, corrosion and wear resistance properties [J]. *Journal of Alloys and Compounds*, 2009, 468: 546–552.
- [3] LEKKA M, ZANELLA C, KLORIKOWSKA A, BONORA P L. Scaling-up of the electrodeposition process of nano-composite coating for corrosion and wear protection [J]. *Electrochimica Acta*, 2010, 55: 7876–7883.
- [4] PENG X, LI T, WU W. Effect of La<sub>2</sub>O<sub>3</sub> particles on the oxidation of electrodeposited nickel films [J]. *Oxidation of Metals*, 1999, 51: 291–315.
- [5] PENG X, LI T, WU W, PAN W P. Effect of La<sub>2</sub>O<sub>3</sub> particles on microstructure and cracking-resistance of NiO scale on electrodeposited nickel films [J]. *Materials Science and Engineering A*, 2001, 298: 100–109.
- [6] QU N S, ZHU D, CHAN K C. Fabrication of Ni–CeO<sub>2</sub> nanocomposite by electrodeposition [J]. *Scripta Materialia*, 2006, 54: 1421–1425.
- [7] XU Y J, LIU H B, LAN M M, LI J S, LI H. Effect of different electrodeposition methods on oxidation resistance of Ni–CeO<sub>2</sub> nanocomposite coating [J]. *Surface and Coatings Technology*, 2010, 204: 3539–3545.
- [8] ZHANG Hai-jun, ZHOU Yue-bo, SUN Jian-feng. Preparation and oxidation behaviour of electrodeposited Ni–CeO<sub>2</sub> nanocomposite coating [J]. *Transactions of Nonferrous Metals Society of China*, 2013, 23(7): 2011–2020.
- [9] ZHOU Y B, SUN J F, WANG S C, ZHANG H J. Oxidation of an electrodeposited Ni–Y<sub>2</sub>O<sub>3</sub> composite film [J]. *Corrosion Science*, 2012, 63: 351–357.
- [10] PFEIL L B, GRIFFITHS W T. Improvement in heat-resisting alloys: UK Patent, 459848 [P]. 1937–05–18.
- [11] MOON D P. Role of reactive elements in alloy protection [J]. *Materials Science and Technology*, 1989, 5: 754–763.
- [12] PINT B A. Experimental observations in support of the dynamic segregation theory to explain the reactive-element effect [J]. *Oxidation of Metals*, 1996, 45: 1–37.
- [13] CZERWINSKI F, SZPUNAR J A, SMELTZER W W. Steady-stage growth of NiO scales on ceria-coated polycrystalline nickel [J]. *J Electrochem Society*, 1996, 143: 3000–3007.
- [14] CZERWINSKI F, SZPUNAR J A. The nanocrystalline ceria sol-gel coatings for high temperature application [J]. *J Sol-Gel Sci Technol*, 1997, 9: 103–114.
- [15] ZHOU Y B, QIAN B Y, ZHANG H J. Al particles size effect on the microstructure of the co-deposited Ni–Al composite coatings [J]. *Thin Solid Films*, 2009, 517: 3287–3291.
- [16] WAGNER C. Type of reaction on the oxidation of alloys [J]. *Z Elektrochem*, 1959, 63: 772–782.
- [17] ATKINSON H V, TAYLOR R I, GOODE P D. Transport processes in the oxidation of Ni studied using tracers in growing NiO scales [J]. *Oxidation of Metals*, 1979, 13: 519–543.
- [18] ATKINSON H V. Evolution of grain structure in nickel oxide scales [J]. *Oxidation of Metals*, 1987, 28: 353–389.
- [19] PERALDI R, MONCEAU D, PIERAGGI B. Correlations between growth kinetics and microstructure for scales formed by high-temperature oxidation of pure nickel. I: Morphologies and microstructures [J]. *Oxidation of Metals*, 2002, 58: 249–273.
- [20] PERALDI R, MONCEAU D, PIERAGGI B. Correlations between growth kinetics and microstructure for scales formed by high-temperature oxidation of pure nickel. II: Growth kinetics [J]. *Oxidation of Metals*, 2002, 58: 275–295.
- [21] HINDAM H M, WHITTLE D. Peg formation by short-circuit diffusion in Al<sub>2</sub>O<sub>3</sub> scales containing oxide dispersions [J]. *J Electrochem Society*, 1982, 129: 1147–1149.
- [22] TAN X, PENG X, WANG F. The mechanism for self-formation of a CeO<sub>2</sub> diffusion barrier layer in an aluminide coating at high temperature [J]. *Surface and Coatings Technology*, 2013, 224(15): 62–70.
- [23] SREEDHAR V, DAS J, MITRA R, ROY S K. Influence of superficial CeO<sub>2</sub> coating on high temperature oxidation behavior of Ti–6Al–4V [J]. *Journal of Alloys and Compounds*, 2012, 519: 106–111.
- [24] HAUGSRUD R. On the effects of surface coatings on the high-temperature oxidation of nickel [J]. *Corrosion Science*, 2003, 45: 1289–1311.
- [25] JACKSON R W, LEONARD J P, NIEWOLAK L, QUADAKKERS W J, MURRAY R, ROMANI S, TATLOCK G J, PETTIT F S, MEIER G H. Analysis of the reactive element effect on the oxidation of ceria doped nickel [J]. *Oxidation of Metals*, 2012, 78: 197–210.

## La<sub>2</sub>O<sub>3</sub>/CeO<sub>2</sub> 颗粒尺寸对 Ni-La<sub>2</sub>O<sub>3</sub>/CeO<sub>2</sub> 复合电镀层高温氧化性能的影响

孟君晟<sup>1,2</sup>, 吉泽升<sup>2</sup>

1. 黑龙江科技大学 材料科学与工程学院, 哈尔滨 150022;
2. 哈尔滨理工大学 材料科学与工程学院, 哈尔滨 150040

**摘 要:** 通过向普通硫酸镍电镀液中添加一定含量的微米或纳米 La<sub>2</sub>O<sub>3</sub>/CeO<sub>2</sub> 颗粒, 采用复合电镀制备微米或纳米 La<sub>2</sub>O<sub>3</sub>/CeO<sub>2</sub> 颗粒分布的 Ni 基复合镀层, 并研究 La<sub>2</sub>O<sub>3</sub>/CeO<sub>2</sub> 颗粒尺寸对 Ni-La<sub>2</sub>O<sub>3</sub>/CeO<sub>2</sub> 复合镀层在 1000 °C 抗氧化性能的影响。结果表明: 与普通 Ni 镀层相比, Ni-La<sub>2</sub>O<sub>3</sub>/CeO<sub>2</sub> 复合镀层中的 La<sub>2</sub>O<sub>3</sub>/CeO<sub>2</sub> 颗粒通过溶解扩散进入氧化膜中, 阻碍 Ni 的外扩散, 从而降低氧化速度; 此外, 与 La<sub>2</sub>O<sub>3</sub>/CeO<sub>2</sub> 纳米颗粒相比, La<sub>2</sub>O<sub>3</sub>/CeO<sub>2</sub> 微米颗粒在氧化初期还起到扩散障碍层的作用, 对阻碍 Ni 的外扩散具有更强的作用。

**关键词:** Ni 基复合镀层; 电沉积; 高温氧化; La<sub>2</sub>O<sub>3</sub>; CeO<sub>2</sub>; 活性元素效应; 氧化机理

(Edited by Wei-ping CHEN)